IEEE Access
Multidisciplinary | Rapid Review | Open Access Journal

Received August 12, 2019, accepted August 26, 2019, date of publication September 4, 2019,
date of current version September 20, 2019.

Digital Object Identifier 10.1109/ACCESS.2019.2939234

Compact Dual-Band Dual-Polarized Base-Station Antenna Array With a Small Frequency Ratio Using Filtering Elements

WEN DUAN[1], YUN FEI CAO[1], YONG-MEI PAN[1], (Senior Member, IEEE), ZHI XING CHEN[1,2], AND XIU YIN ZHANG[1], (Senior Member, IEEE)

[1]School of Electronic and Information Engineering, South China University of Technology, Guangzhou 510641, China
[2]Shenglu Communication Technology Company Ltd., Foshan 528100, China

Corresponding author: Xiu Yin Zhang (zhangxiuyin@scut.edu.cn)

ABSTRACT This paper presents a compact dual-band ±45° dual-polarized base-station array based on embedded filtering elements. The proposed antenna array consists of 9 dual-band antenna units, which operate at the lower band (LB) of 790–862 MHz and the higher band (HB) of 880–960 MHz with a small frequency spacing. In each unit, one antenna element is embedded into the other one, featuring a very compact size. To alleviate the serious cross-band mutual coupling between the two elements, the LB patch antenna generates a boresight radiation null at its higher band edge, and the HB element is designed with a band-stop response at its lower band edge. In this way, high cross-band isolation between the two embedded elements can be obtained. For demonstration, a compact dual-band ±45° dual-polarized filtering antenna array with 9 units is designed and fabricated to fit the specification of LB and HB bands ($|S_{11}| < -15$ dB). The overall width of the array is only 280 mm, which is much narrower than that of typical industrial products using two side-by-side sub-arrays (∼576 mm). The measured performance of the antenna array can meet the requirement of base stations.

INDEX TERMS Base-station antenna array, filtering antenna, dual band, mutual coupling reduction, compact size.

I. INTRODUCTION

With the development of mobile communications, multi-band and multi-standard wireless systems are employed. Among these systems, some adjacent frequency bands are allocated to different mobile communication operators. For instance, the band of 880-960 MHz is allocated to one operator and the band of 790-862 MHz is assigned to the other one. Although a wideband antenna array with the corresponding wideband feeding network can cover the frequency band of 790-960 MHz, it cannot be shared by two operators because there is one set of ports which can be only connected to the transceivers of the specific operator. This problem can be solved by using two independent arrays. However, the size is too large. It is difficult for operators to find proper sites with enough volume for installing base-station arrays [1]. So, the compact dual-band dual-polarized antenna arrays with two sets of ports are required to simultaneously support two operators.

In the design of a dual-band antenna array with a small frequency ratio, two typical design methods have been employed. One approach is to use two sub-arrays placed side-by-side, as illustrated in Fig. 1(a). In the case of small frequency ratio for the two bands, i.e., 790-862 MHz and 880-960 MHz, the mutual coupling between the two sub-arrays deteriorates the isolation and radiation patterns. Then, the decoupling network is necessary to improve isolation [2]–[5]. To maintain the radiation patterns, the separation between antenna elements should be increased, which makes the array bulky [6]. The size can be reduced by using the filtering elements [7], [8]. However, they have only single polarization, and the size is still large.

The other approach for a dual-band array design is to use duplexers in series with full-band antennas to realize dual-band performance, as shown in Fig. 1(b). A duplexer is

The associate editor coordinating the review of this article and approving it for publication was Choon Ki Ahn.

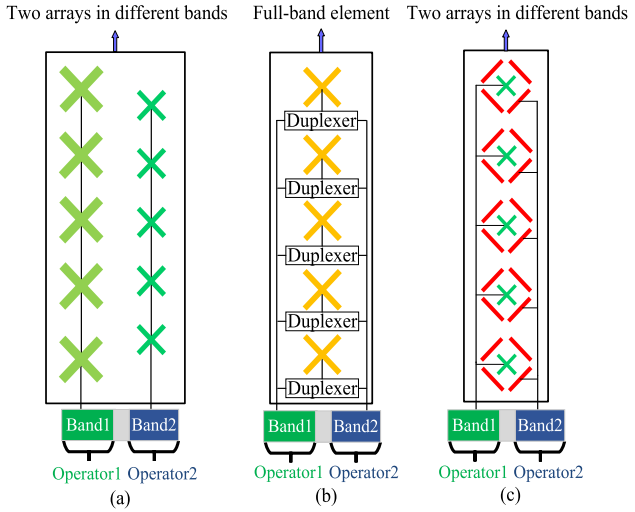

FIGURE 1. Dual-band antenna arrays in two close bands. (a) Two sub-arrays placed side-by-side; (b) each wideband element with a duplexer; (c) embedded dual-band antenna elements.

cascaded with each wideband element. Two sets of feeding networks for the two bands are employed to control the downtilt independently, which is necessary for the wireless network optimization [9]. If the two frequency bands are very close to each other, it is very difficult to design the duplexer with acceptable performance, compact size, low cost and weight [1]. If the duplexer is designed on the printed circuit board (PCB), the insertion loss is usually higher than 2 dB because of close frequency spacing which results in the drastic degradation of the array radiation gain. Alternately, cavity duplexers featuring lower insertion loss can be used, but they are too expensive and heavy in this case.

To realize size and cost reduction, a novel embedding scheme for dual-band arrays with a small frequency spacing is proposed in this paper, as shown in Fig. 1(c). Although the embedding scheme have been used, it can be only applied to dual-band arrays with a large frequency ratio, i.e., 824–960 MHz and 1710–2170 MHz. In this case, the mutual coupling between two elements is very low because of the large frequency spacing [10]–[13]. In case of a small frequency spacing, the strong cross-band mutual coupling affects isolation and degrades antenna gain. To solve this problem, embedded dual-band dual-polarized filtering elements with high selectivity are designed in this paper. Although much work on dual-polarized filtering antennas was conducted [14]–[19], the frequency selectivity was not good enough to suppress the cross-band coupling when two operating bands are close, or the structures were not suitable for the embedding schemes [16]. For the first time, this work proposes an embedded dual-band dual-polarized filtering antenna pair with high isolation and then uses it to realize a compact and low-cost dual-polarized antenna array operating in two close bands. The operating mechanism is analyzed in detail, and the antenna element pair and array are designed. The simulated and measured results are presented as well.

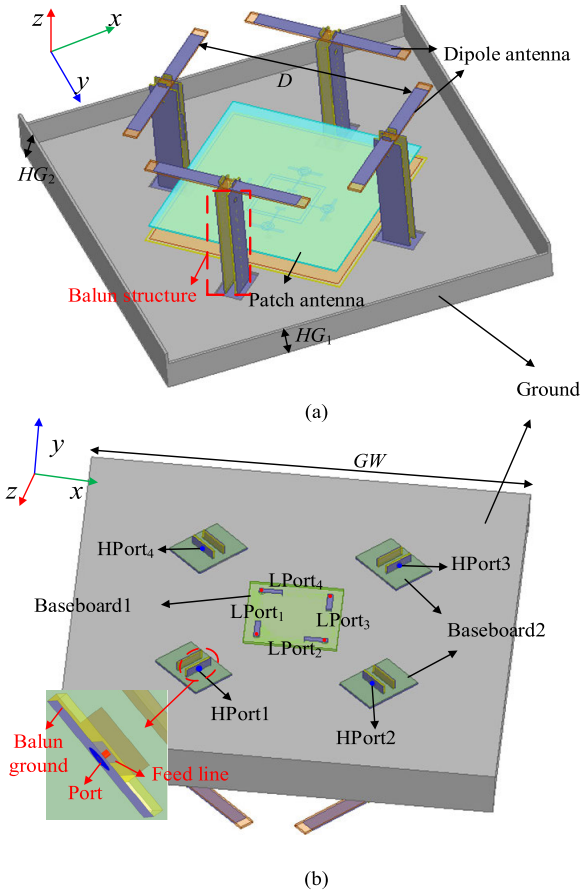

FIGURE 2. 3-D configuration of the proposed dual-band dual-polarized filtering antenna unit. (a) Above the ground; (b) below the ground.

II. ANTENNA UNIT DESIGN

A. CONFIGURATION OF THE PROPOSED ANTENNA UNIT

Fig. 2 illustrates the 3-D configuration of the proposed dual-band dual-polarized filtering antenna unit. It mainly consists of a ground reflector, a patch antenna operating at 790–862 MHz and four dipole antennas at 880–960 MHz around the patch antenna. To optimize the front-to-back ratio and cross-polarization level, four metal walls with different heights (HG_2 and HG_1) are added around the square ground with the sidelength of GW. The baseboard1 below the ground is for fixing the patch antenna and connecting the coaxial cable, and the baseboard2 is for dipole antennas. These baseboards (Rogers 4533) have the same permittivity of $\varepsilon_r = 3.3$ and thickness of $t = 1.524$ mm.

The configuration of the patch antenna operating at 790-862 MHz is shown in Fig. 3. With reference to the figures, the square stacked patch (Fig. 3(a)) with a sidelength of PL_1 is an aluminum sheet with a thickness of 1mm, whereas the driven patch (Fig. 3(d)) with the sidelength of PL_2 and the feeding circuit (Fig. 1(e)) are fabricated on the top and bottom surfaces of the substrate1, respectively. The substrate1 has a permittivity of $\varepsilon_r = 3.3$, thickness of $t = 0.762$ mm and size of $SubL \times SubL$. An air gap with the height of h_2 is introduced

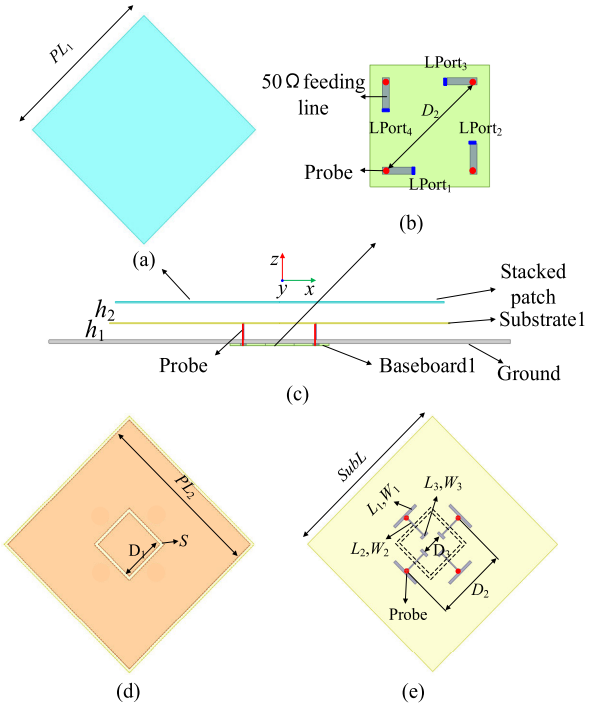

FIGURE 3. Configuration of the proposed dual-polarized filtering patch antenna. (a) Stacked patch; (b) feeding ports; (c) side view; (d) driven patch; (e) feeding lines.

between the two patches mainly for optimizing the antenna bandwidth. Another air gap between the driven patch and ground with the height of h_1 is for impedance matching.

The feeding structure of the patch antenna consists of I-shaped coupling feeding lines on the backside of the substrate1 (Fig. 3(e)), the 50-Ω feeding lines on the backside of the baseboard1 (Fig. 3(b)) and four probes. These probes connect the I-shaped coupling feeding lines and the 50Ω feeding lines, which are denoted by the red dot. Due to the strong inductance of the probes, the square ring slot with the width of s on the driven patch (Fig. 3(d)) and the I-shaped coupling feeding line provide a capacitance for impedance matching. The specific I-shaped feeding line is designed as a stepped-impedance line with different widths, as shown in Fig. 3(e). In Fig. 3(b), Lport1 and Lport3 are fed with the same amplitude but differential phase for −45° polarization, while the Lport2 and Lport4 are for +45° polarization. The isolation between the two polarizations can be enhanced by using the differential feeding method [20], [21]. The distance D_2 between two probes is introduced to control the impedance. The detailed dimensions of the proposed patch antenna are listed in Table 1.

Fig. 4 shows the element operating at 880-960 MHz. It consists of four dipole antennas in a square, acting as a dual-polarized element [13]. Dipole1 and dipole3 (or dipole2 and dipole4) are symmetrically placed. Dipole1 and dipole3 are fed with the same amplitude and phase for −45° polarization, while dipole2 and dipole4 are for +45° polarization. The distance D between the two mirror symmetrical dipoles is

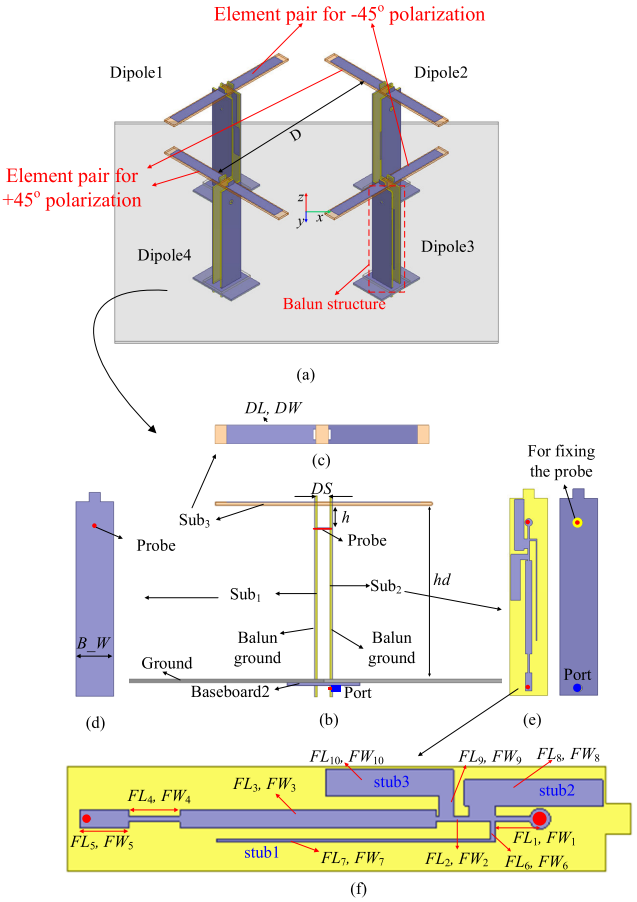

FIGURE 4. Configuration of the proposed dual-polarized filtering dipole antenna. (a) 3-D configuration; (b) side view; (c) arm of the dipole; (d) balun on the left; (e) balun on the right; (f) balun feeding circuit.

TABLE 1. Parameters of the proposed antenna (Unit: MM).

HG_1	HG_2	D	h_1	h_2	PL_1	PL_2	D_1	D_2
30	60	158.3	11	10	143	142	36	62
D_3	S	$SubL$	L_1	W_1	L_2	W_2	L_3	W_3
16.4	2.5	146	25	1.8	22	0.9	8	1.8
DL	DW	DS	B_W	hd	h	FW_1	FL_1	FW_2
51.5	8.5	7	20	85	13.7	1	8.75	1
FL_2	FW_3	FL_3	FW_4	FL_4	FW_5	FL_5	FW_6	FL_6
10.5	4	40	2.5	9	3.5	9.5	1	4
FW_7	FL_7	FW_8	FL_8	FW_9	FL_9	FW_{10}	FL_{10}	GW
0.6	54.6	4.5	26	3	4	5.5	25	280

related to the beamwidth for HB element. According to the array synthesis theory [22], the beamwidth will be widened if D is decreased.

The configuration of the single dipole antenna is also shown in Fig. 4. Just like a traditional dipole antenna, the proposed filtering dipole consists of a half-wavelength radiation arm, a balun, and a ground. The radiation arm printed on the top of the substrate in Fig. 4(c) is two rectangle sheets with a width of DW and length of DL. The balun is composed of

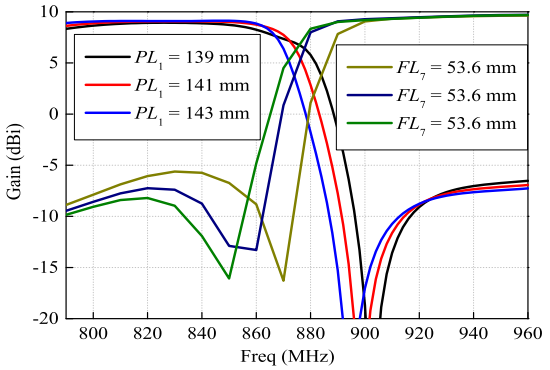

FIGURE 5. Effect of the size of stacked patch and open stub on the realized gain when the proposed antenna is excited in +45° polarization.

two substrates Sub1 and Sub2 which are connected together by a metal probe with a distance of h from the dipole arm, as shown in Fig. 4(b) and (d)-(f). These two substrates are connected to the dipole arm and the baseboard2 in Fig. 4(b). All the substrates for dipole antenna have the permittivity of $\varepsilon_r = 3.3$ and thickness of $t = 1.524$ mm. The copper sheets on the left side of the substrate Sub1 and the right side of Sub2 are as the balun ground. The feeding line on the left side of Sub2 is the balun feeding network with a bandstop response. It consists of a stepped-impedance feeding line with three stub lines, as shown in Fig. 4(f). The stub1 with the width of FW_7 and length of FL_7 is designed to generate a bandstop response at the lower band edge. Two other stubs with the width of FW_8 and FW_{10} are used for impedance matching. The detailed dimensions of the proposed dipole antenna are listed in Table 1.

B. ANALYSIS OF FILTERING PERFORMANCE OF THE PROPOSED PATCH AND DIPOLE ANTENNA

The filtering performance for the patch antenna can be obtained by the elaborately designed stacked patch, which had been studied in [14], [23]. Fig. 5 shows the gain curves of the proposed dual-band antenna with different sizes of the stacked patch and filtering stub. It can be seen that the low-pass filtering response with a radiation null at the higher band edge is realized, and the selectivity can be controlled by changing the size of the stacked patch. The high-pass filtering response with a radiation null at the lower band edge is observed, and high selectivity can be achieved by choosing the suitable length FL_7 of the stub1 in the balun feeding network. The filtering performance caused by the open-circuited stub line can be explained using the filter theory [24].

Based on the above filtering performance of the proposed patch and dipole antennas, it can be inferred that the mutual coupling between the two designed operating bands can be reduced when the patch antenna and the dipole antennas are combined as a dual-band dual-polarized antenna unit shown in Fig. 2. To verify this, Fig. 6 gives the cross-band isolation comparison between filtering and non-filtering (traditional)

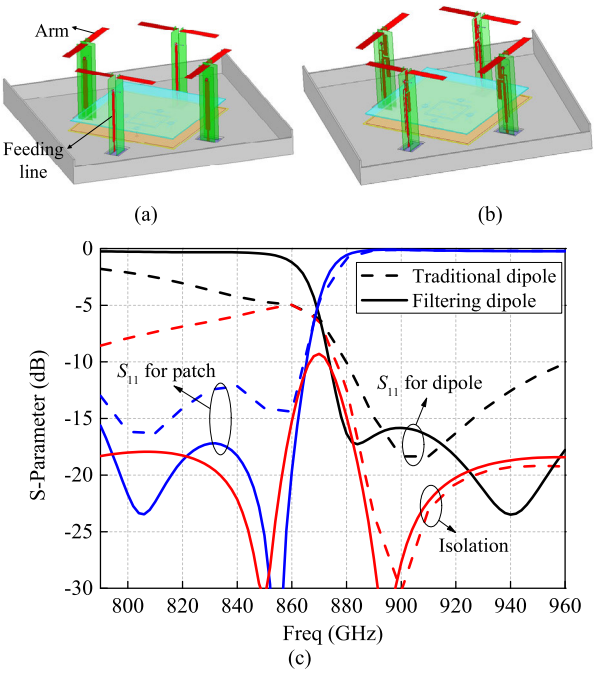

FIGURE 6. Comparison of S-parameters in the same polarization when the HB elements are designed (a) with and (b) without filtering performance.

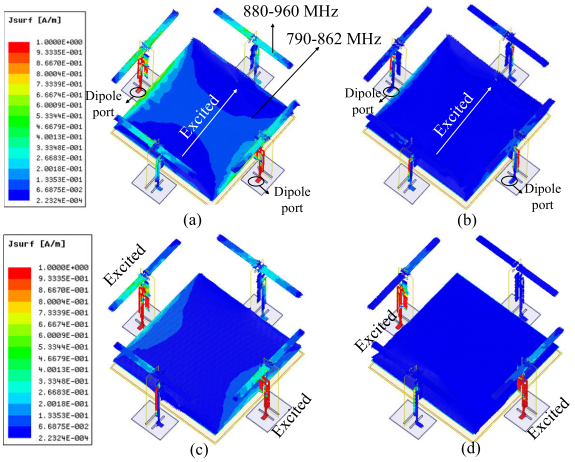

FIGURE 7. Current distribution when patch is excited at (a) 870MHz; (b) 890MHz; when dipole is excited at (c) 870MHz; (d) 890MHz.

HB elements operating at 880-960 MHz. It can be seen that the isolation in the lower operating band is only 5 dB when the traditional dipole is used. Using the proposed filtering element, the isolation is improved to 15 dB. Similarly, the isolation in the higher operating band will be worse if using the non-filtering patch at the lower band. To show the mutual coupling clearly, the current distributions are given in Fig. 7 illustrates that patterns and current distributions when the patch antenna (operating at 790-862 MHz) is excited. As seen, the current at the dipole port is induced when the patch antenna is excited at 870 MHz. The current is very weak when the patch antenna is excited at 890 MHz (radiation

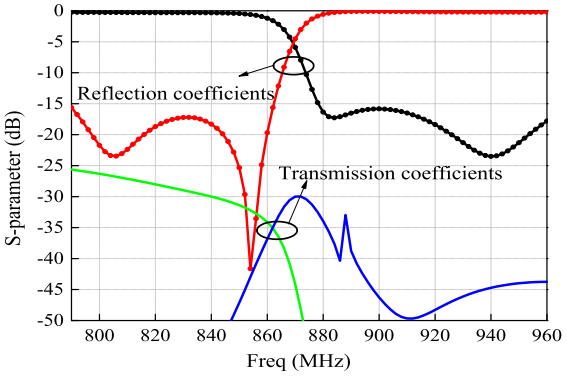

FIGURE 8. Simulated reflection coefficients and isolations of the proposed dual-band filtering antenna unit.

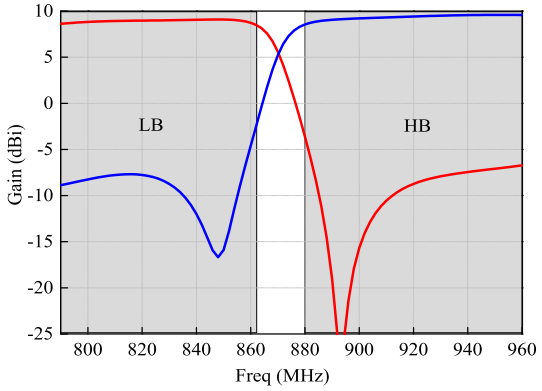

FIGURE 9. Simulated gain of the proposed dual-band filtering antenna unit.

null). Similarly, when the dipole antenna (operating at 880-960 MHz) is excited, the current on the patch edge is induced at 870 MHz, and it is very weak at 850 MHz (radiation null).

C. RESULTS OF THE PROPOSED ANTENNA UNIT

Since high isolation between the two elements can be realized using the filtering antennas, the performance of each operating band can be optimized independently, and the radiation patterns at these two bands have a very slight effect on each other. Fig. 8 shows the simulated reflection coefficients and polarization isolation of the proposed dual-band filtering antenna unit. It can be seen that the impedance bandwidths ($|S_{11}| < -15$ dB) cover the 790-862 MHz and 880-960 MHz bands. Due to the orthogonal structure and feeding method, the polarization isolation of patch antenna is lower than 26 dB, and that of the dipole antenna can reach 33 dB. With reference to the gain curves in Fig. 9, the gain in the lower band ranges from 8.6 dBi to 9.1 dBi and from 8.6 dBi to 9.6 dBi in the higher band. The gain fluctuations are within 1 dB inside both bands, which is reasonable. High selectivity is obtained by the two radiation nulls at 895 MHz and 848 MHz, which are generated by the stacked patch and the balun feeding stub line, respectively. Although the gain at 870 MHz is about 5.5 dBi, it is not in the operating band and does not affect the in-band performance.

Fig.10 shows the simulated radiation patterns in horizontal plane (*xoz*-plane) for the proposed dual-band dual-polarized filtering antenna unit in the $+45°$ polarization state. As can be observed, stable broadside radiation characteristics are obtained across the two passbands. With reference to these figures, the front-to-back (F/B) ratios are more than 28 dB in all the operating frequencies. The cross-polarization level over the co-polarization in the axial direction is at least -18 dB for the patch antenna, and -20 dB for the dipole antenna. In particular, the cross-polarization levels of -13 dB and -18 dB can be found in $\pm 60°$ for the patch and dipole antennas, which is also a key parameter in the base-station antenna array. Moreover, the 3-dB beamwidths in the horizontal plane are $68 \pm 1.5°$ in the lower band and $62 \pm 1°$ in the higher band, which are very stable. Due to the symmetry

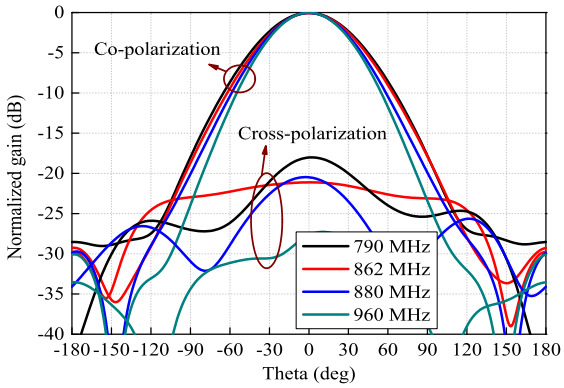

FIGURE 10. Radiation patterns in *xoz*-plane of the proposed dual-band filtering antenna excited in $+45°$ polarization.

of the structure of the proposed antenna, the same radiation performance can be achieved in the $-45°$ polarization state, which is not repeated here for brevity. All the radiation performance and structural stability of the proposed dual-band dual-polarized filtering antenna unit indicate that it is suitable to be a good choice for a base-station antenna array.

III. NINE-UNIT ANTENNA ARRAY DESIGN

Using the dual-band dual-polarized filtering antenna unit, a high gain 9-unit antenna array is implemented for base-station applications in this Section. In the Experiment, the *S*-parameters are measured using an Agilent N5230A network analyzer, and radiation patterns and antenna gains are measured using a Satimo Startlab System.

A. ANTENNA ARRAY STRUCTURE

Fig. 11 shows the structure of 9-unit antenna array. The distance D_4 between antenna units is set to 280 mm, i.e., $0.737\lambda_L$, where λ_L is the free-space wavelength at 790 MHz. The width *GW* of the ground is 280 mm, which is much narrower than that of the industrial product (576 mm) [10]. The length *GL* of the ground is 2522 mm. Vertical metal walls are inserted between antenna units to optimize the

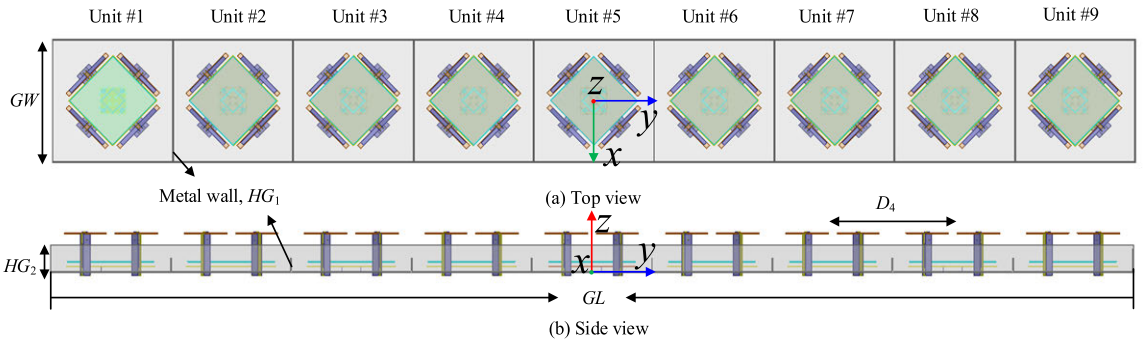

FIGURE 11. Structure of nine-unit antenna array. (a) Top view; (b) side view.

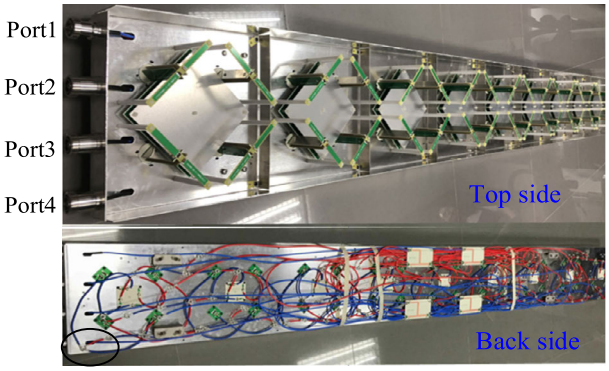

FIGURE 12. Photos of the proposed dual-band dual-polarized filtering antenna array with its feeding networks.

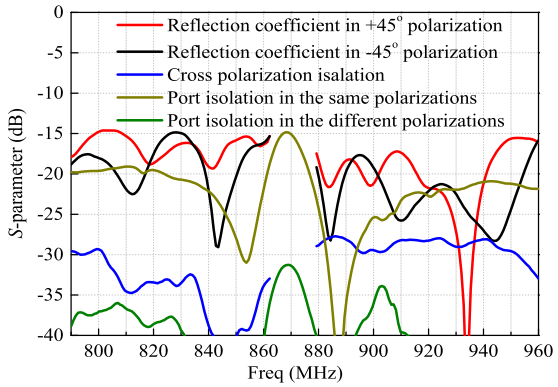

FIGURE 13. Measured reflection coefficients and isolations of the proposed filtering antenna array.

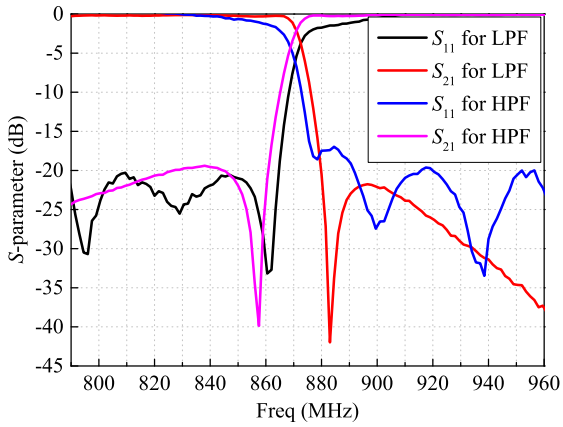

FIGURE 14. Measured results of the required two filters.

front-to-back ratio and cross-polarization level of the antenna array. Fig. 12 shows the photograph of the fabricated dual-band dual-polarized filtering antenna array with its feeding networks. There are four inputs as shown in Fig. 12. Port 1 and 2 are the inputs for patch antenna array, and port 3 and 4 are for the dipole antenna array. Among them, port 1 and 3 are for $-45°$ polarization, whereas port 2 and 4 are for $+45°$ polarization.

B. RESULT OF THE ANTENNA ARRAY

Fig. 13 shows the measured reflection coefficients and isolations of the proposed dual-band dual-polarized filtering antenna array. The reflection coefficients of lower than -15 dB can be seen in the two operating bands with dual polarization. The in-band polarization isolations are 29 dB for 790-862 MHz and 27.6 dB for 880-960 MHz. Due to the filtering performance of the proposed antenna unit, the isolations between two bands are 19 dB in the same polarization and 32 dB in the orthogonal polarization. The isolation of 19 dB has a limited effect on the radiation performance of dual-band antenna array. In the base-station system, the isolation between different bands is usually more than 28 dB. A filter needs to be connected to the input ports to further improve the out-of-band rejection.

Fig. 14 shows the measured results of the filters (a low-pass filter (LPF) and a high-pass filter (HPF)). The reflection coefficients of -17 dB can be obtained in both two filters. The transmission coefficients are -0.3 dB in operating bands and -17 dB in the suppression band. It should be mentioned that the two filters with the required performance can be realized easily. They are simpler, cheaper and lighter than the traditional duplexer with acceptable performance. Fig. 15 shows the measured isolation between the two operating bands when the two filters are connected to the input ports of the proposed dual-band antenna array. It can be observed that the isolation

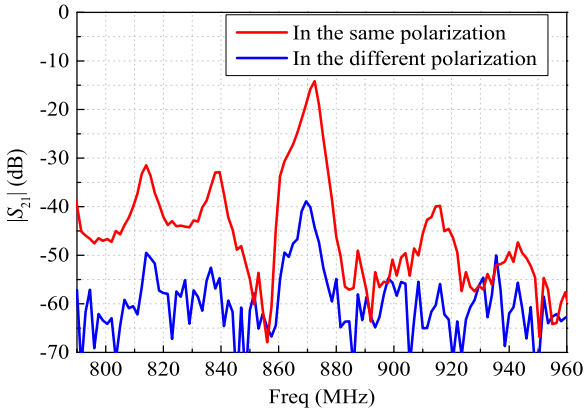

FIGURE 15. Measured isolations between different operating bands after adding the filters.

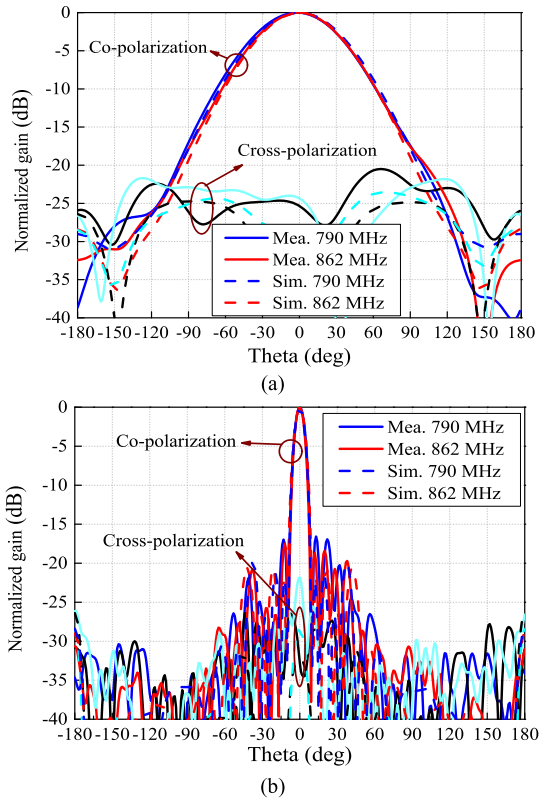

FIGURE 16. Simulated and measured radiation patterns when the patch antenna array is excited for +45° polarization. (a) H-plane; (b) V-plane.

of 32 dB is achieved, which can meet the requirement of base-station systems.

Fig. 16 shows the simulated and measured radiation patterns of the proposed dual-band dual-polarized filtering antenna array when the LB patch antenna array is excited in +45° polarization. As can be observed, stable broadside radiation characteristics are obtained across the entire passband (790-862 MHz). The simulated 3-dB beamwidths are 67 ± 1.5° in the horizontal plane (H-plane, *xoz*-plane) and 8.1 ± 0.4° in the vertical plane (V-plane, *yoz*-plane).

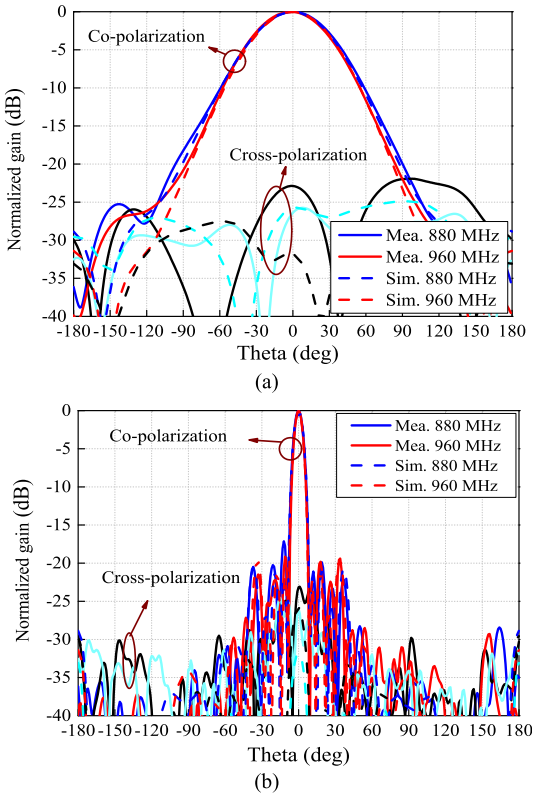

FIGURE 17. Measured radiation patterns when the dipole antenna array is excited for +45° polarization. (a) H-plane; (b) V-plane.

The measured 3-dB beamwidths are 68° ± 2° and 8 ± 0.2°. The simulated and measured front-to-back ratios are both higher than 26 dB. The simulated cross-polarization level can reach −28 dB, and the measured one is −22 dB. The simulated first upper side-lobe level can be improved to −21 dB for the two operating bands by setting the power magnitude ratio of nine antenna units to 1.5:1.5:2.5:2.5:4:2.5:2.5:1.5:1.5 (unit #1 to #9). The measured upper side-lobe level is −17 dB. The little difference between the simulated and measured radiation patterns is mainly due to the processing error.

The simulated and measured radiation patterns of the dipole antenna array (880-960 MHz) for +45° polarization are depicted in Fig. 17. It can be seen that the simulated 3-dB beamwidths are 60.5 ± 1° in *xoz*-plane and 7.2 ± 0.4° in *yoz*-plane. The measured 3-dB beamwidths are 62° ± 2° and 7.5 ± 0.1°. The measured 3-dB beamwidths of the dual-band dual-polarized antenna array are summarized in Fig. 18. The simulated and measured front-to-back ratios are both higher than 29 dB. The simulated cross-polarization level can reach −26 dB, and the measured one is −22 dB. The first upper side- lobe levels are −17 dB.

Fig. 19 shows the simulated and measured gains of the proposed dual-band dual-polarized antenna array. The simulated gains in the LB and HB bands are higher than 17.4 dBi and 18 dBi, respectively, which agree with the theoretically predicted ones [22]. The measured gains are ∼16 dBi for

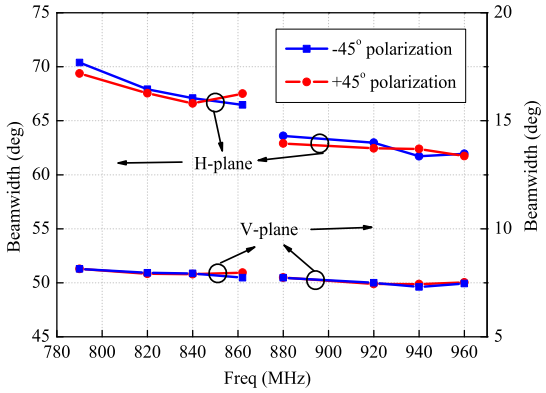

FIGURE 18. Measured 3-dB beamwidths of the proposed dual-band dual-polarized antenna array.

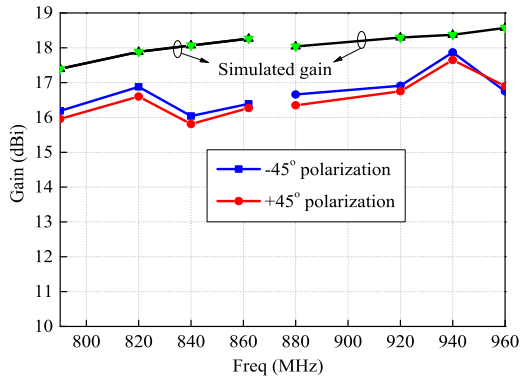

FIGURE 19. Gains of the proposed dual-band dual-polarized antenna array.

the lower band and ∼16.5 dBi for the higher band. The difference of 1.5 dB between simulation and measurement is mainly caused by the line loss and fabrication error. The gain instability and the difference between the two polarizations in measurement are due to the measuring and welding errors.

C. COMPARISON

To further highlight the advantages of the proposed antenna and array, several latest dual-polarized filtering antennas, as well as six dual-band base-station antenna arrays are compared as tabulated in Table 2 and 3, respectively. Firstly, some important parameters for filtering antenna, including bandwidth and frequency selectivity are presented in Table 2. Compared with the other dual-polarized filtering antennas [14], [15], [18], [19], the proposed antenna exhibits higher roll-off rate. Thus, these designs cannot fulfill the requirement of cross-band isolation reduction for two close frequency bands. Compared with the design in [16], the proposed design exhibits higher gain since it does not use extra resonators which introduce extra loss.

Table 3 compares the proposed array with some other dual-band base-station antenna arrays. With the same operating frequencies, the dual-band dual-polarized antenna array

TABLE 2. Comparison with previous dual-polarized filtering antennas.

Ref.	Antenna type	(Null 1) BW (Null 2) (GHz)			Gain (dBi)
[14]	Patch	(2.0)	2.49-2.69	(3.6)	9
[15]	Dipole	(1.2)	1.66-2.73	(2.9)	8.1
[16]	Slot array (2*2)	(36)	36.8-37.33	(38)	9
[18]	Patch	(N.A)	1.72-1.86	(N.A)	7
		(N.A)	1.95-2.12	(N.A)	7.2
[19]	Dipole	(2.5)	3.40-3.80	(4.5)	9
This work	Patch	(None)	0.79-0.862	(0.892)	9
	Dipole	(0.85)	0.88-0.96	(None)	9

Null 1 is the radiation null in the lower band-edge, Null 2 is the radiation null in the higher band-edge. BW is the operating bandwidth.

TABLE 3. Comparison with previous dual-band antenna arrays.

Ref.	Polarization	Frequency	Array width	F/B Ratio (dB)
[6]	Dual	790-862 MHz & 880-960 MHz	576mm ($1.51\lambda_L$)	27
[7]	Single	1710-1880 MHz & 1920-2170 MHz	206mm ($1.41\lambda_L$)	20
[8]	Single	1710-1880 MHz & 1920-2170 MHz	165mm ($0.92\lambda_L$)	15
[11]	Dual	800-990 MHz & 1660-2210 MHz	300mm ($0.8\lambda_L$)	18
[12]	Dual	790-960 MHz & 1710-2170 MHz	255mm ($0.671\lambda_L$)	25
[13]	Dual	770-980 MHz & 1650-2900 MHz	280mm ($0.737\lambda_L$)	20
This work	Dual	790-862 MHz & 880-960 MHz	280mm ($0.737\lambda_L$)	26

λ_L is the wavelength at the lowest operating frequency.

product from industry [6] consists of two sub-arrays placed side by side. The width of 576 mm ($1.51\lambda_L$) is twice that of the proposed one (280 mm). The smaller size will greatly reduce the practical installation cost. The designs in [7], [8] are singly polarized ones and cannot be employed in the proposed design. Although the similar width for dual-band antenna arrays is obtained in [11]–[13], the two operating frequency bands are far away from each other and the mutual coupling is very low. And they are not suitable for the close frequency bands with a strong mutual coupling.

IV. CONCLUSION

A novel compact and low-cost dual-polarized filtering antenna array operating in two close bands with the satisfying performance for base-station systems has been investigated in this paper. Two antenna elements with low-pass and high-pass filtering performance have been designed and integrated into one antenna array unit. Small ground width and high port isolation have been realized by using the proposed antenna unit. An antenna array with nine units has been fabricated and measured. The overall width of the array is only 280 mm, which is much narrower than that of typical industrial products (∼576 mm) with similar performance. High gains and stable radiation patterns have been achieved in the designed two passbands. With the features of compact size, simple

structure, low cost and weight, the proposed nine-unit antenna array is suitable for practical base-station applications. It is worth mentioning that the proposed decoupling method can also be used to design antennas at other frequency bands, including 5G frequency bands.

REFERENCES

[1] (May 2012). *MIMO and Smart Antennas for 3G and 4G Wireless Systems—Practical Aspects and Deployment Considerations*. [Online]. Available: https://www.gsma.com/spectrum/wp-content/uploads/2012/03/mimo.pdf
[2] L. Zhao, F. Liu, X. Shen, G. Jing, Y.-M. Cai, and Y. Li, "A high-pass antenna interference cancellation chip for mutual coupling reduction of antennas in contiguous frequency bands," *IEEE Access*, vol. 6, pp. 38097–38105, 2018.
[3] L. Zhao and K.-L. Wu, "A dual-band coupled resonator decoupling network for two coupled antennas," *IEEE Trans. Antennas Propag.*, vol. 63, no. 7, pp. 2843–2850, Jul. 2015.
[4] L. Zhao, K.-W. Qian, and K.-L. Wu, "A cascaded coupled resonator decoupling network for mitigating interference between two radios in adjacent frequency bands," *IEEE Trans. Microw. Theory Techn.*, vol. 62, no. 11, pp. 2680–2688, Nov. 2014.
[5] K.-W. Qian, "A compact LTCC decoupling-network based on coupled-resonator for antenna interference suppression of adjacent frequency bands," *IEEE Access*, vol. 6, pp. 25485–25492, 2019.
[6] Kathrein USA, Greenway Plaza II. (2015). *Data Sheet 80010656*. [Online]. Available: http://www.kathreinusa.com/wp-content/uploads/2015/12/80010647V01.pdf
[7] Y. Zhang, X. Y. Zhang, L.-H. Ye, and Y.-M. Pan, "Dual-band base station array using filtering antenna elements for mutual coupling suppression," *IEEE Trans. Antennas Propag.*, vol. 64, no. 8, pp. 3423–3430, Aug. 2016.
[8] M. Li, Q. Li, B. Wang, C. Zhou, and S. Cheung, "A miniaturized dual-band base station array antenna using band notch dipole antenna elements and AMC reflectors," *IEEE Trans. Antennas Propag.*, vol. 66, no. 6, pp. 3189–3194, Jun. 2018.
[9] X. Li, R. W. Heath, Jr., K. Linehan, and R. Butler, "Metrocell antennas: The positive impact of a narrow vertical beamwidth and electrical downtilt," *IEEE Veh. Technol. Mag.*, vol. 10, no. 3, pp. 51–59, Sep. 2015.
[10] Y. Cui, R. Li, and P. Wang, "Novel dual-broadband planar antenna and its array for 2G/3G/LTE base stations," *IEEE Trans. Antennas Propag.*, vol. 61, no. 3, pp. 1132–1139, Mar. 2013.
[11] S. Chen and K.-M. Luk, "High performance dual-band dual-polarized magneto-electric dipole base station antenna," in *Proc. Asia–Pacific Microw. Conf. (APMC)*, Nov. 2014, pp. 321–323.
[12] Y. He, W. Tian, and L. Zhang, "A novel dual-broadband dual-polarized electrical downtilt base station antenna for 2G/3G applications," *IEEE Access*, vol. 5, pp. 15241–15249, 2017.
[13] H. Huang, Y. Liu, and S. Gong, "A novel dual-broadband and dual-polarized antenna for 2G/3G/LTE base stations," *IEEE Trans. Antennas Propag.*, vol. 64, no. 9, pp. 4113–4118, Sep. 2016.
[14] W. Duan, X. Y. Zhang, Y.-M. Pan, J.-X. Xu, and Q. Xue, "Dual-polarized filtering antenna with high selectivity and low cross polarization," *IEEE Trans. Antennas Propag.*, vol. 64, no. 10, pp. 4188–4195, Oct. 2016.
[15] C. F. Ding, X. Y. Zhang, Y. Zhang, Y.-M. Pan, and Q. Xue, "Compact broadband dual-polarized filtering dipole antenna with high selectivity for base-station applications," *IEEE Trans. Antennas Propag.*, vol. 66, no. 11, pp. 5747–5756, Nov. 2018.
[16] H. Chu and Y.-X. Guo, "A filtering dual-polarized antenna subarray targeting for base stations in millimeter-wave 5G wireless communications," *IEEE Trans. Compon., Packag., Manuf. Technol.*, vol. 7, no. 6, pp. 964–973, May 2017.
[17] C.-X. Mao, S. Gao, Y. Wang, Q. Luo, and Q.-X. Chu, "A shared-aperture dual-band dual-polarized filtering-antenna-array with improved frequency response," *IEEE Trans. Antennas Propag.*, vol. 65, no. 4, pp. 1836–1844, Apr. 2017.
[18] J.-F. Li, D.-L. Wu, G. Zhang, Y.-J. Wu, and C.-X. Mao, "Compact dual-polarized antenna for dual-band full-duplex base station applications," *IEEE Access*, vol. 6, pp. 72761–72769, 2019.
[19] C. Hua, R. Li, Y. Wang, and Y. Lu, "Dual-polarized filtering antenna with printed Jerusalem-cross radiator," *IEEE Access*, vol. 6, pp. 9000–9005, 2018.
[20] Y. P. Zhang and J. J. Wang, "Theory and analysis of differentially-driven microstrip antennas," *IEEE Trans. Antennas Propag.*, vol. 54, no. 4, pp. 1092–1099, Apr. 2006.
[21] Q. Xue, S. W. Liao, and J. H. Xu, "A differentially-driven dual-polarized magneto-electric dipole antenna," *IEEE Trans. Antennas Propag.*, vol. 61, no. 1, pp. 425–430, Jan. 2013.
[22] C. A. Balanis, *Antenna Theory: Analysis and Design*, 3rd ed. New York, NY, USA: Wiley, 2005.
[23] X. Y. Zhang, W. Duan, and Y.-M. Pan, "High-gain filtering patch antenna without extra circuit," *IEEE Trans. Antennas Propag.*, vol. 63, no. 12, pp. 5883–5888, Dec. 2015.
[24] D. M. Pozar, *Microwave Engineering*, 3rd ed. New York, NY, USA: Wiley, 2005.